Equine Veterinary Education

EQUINE VETERINARY EDUCATION
Equine vet. Educ. (2019) •• (••) ••-••
doi: 10.1111/eve.13088

Review Article

A review of normal radiographical variants commonly mistaken for pathological findings in horses

F. E. Hinkle*†, *S. A. Johnson*‡, *K. T. Selberg*† and *M. F. Barrett*†

†*Department of Environmental and Radiological Health Sciences, Colorado State University; and* ‡*Department of Clinical Sciences, Colorado State University, Fort Collins, Colorado, USA*
**Corresponding author email: myra.barrett@colostate.edu*

Keywords: horse; radiography; normal variants

Summary

A normal variant is an atypical finding present in a percentage of the population that generally has no clinical significance and is considered within the spectrum of normal findings. Normal variants are recognised upon gross anatomical dissection and also observed radiographically. Understanding the range of normal variants is essential for proper radiographical interpretation. This ensures that these variants are not mistaken for pathological lesions and helps avoid radiographical misdiagnosis. Common sites of normal anatomical variation in the foot, pastern, carpus, tarsus, elbow, shoulder and axial skeleton are reviewed.

Introduction

Accurate radiographical interpretation requires more than recognition of abnormalities. A solid understanding of normal anatomical and incidental variants is crucial to avoid misinterpretation of radiographical findings. A normal variation commonly occurs in a typical location without other evidence of concurrent pathological bone change, such as sclerosis or lysis. The misdiagnosis of a normal variant as a significant lesion can result in deleterious consequences, including inappropriate case management, unnecessary surgery or incorrect client counsel in the prepurchase examination scenario. In addition, identifying a normal variant as pathological precludes accurate diagnosis of the true source of lameness. The following is a review of normal radiographical variants that are commonly mistaken for pathological abnormalities.

Distal phalanx, navicular bone and distal interphalangeal joint

Numerous anatomical variants of the foot have been described. These include normal variation in the extensor process shape, separate centres of ossification of the palmar processes, ossification of the ungual cartilages, separate centres of ossification of the ungual cartilages and the crena marginalis solaris (Becht *et al.* 2001). The dorsal margin of the distal interphalangeal joint is a common area of misinterpretation within the foot. The dorsodistal aspect of the middle phalanx and extensor process of the distal phalanx can have variable conformation. In some horses, these surfaces are smooth and rounded, whereas in others the margins are pointed with sharp contours (**Fig 1**). In some cases, it can be challenging to differentiate the sharply pointed normal variant from an osteophyte and normal variants can be easily overinterpreted as degenerative changes. The pointed, sharp contour variant of the distodorsal middle phalanx will generally be bilaterally symmetrical without other evidence of joint disease, such as additional sites of osteophytosis, joint capsule enthesopathy, subchondral bone sclerosis or evidence of distal interphalangeal joint effusion. Concurrent osteophytes on the distopalmar/plantar aspect of the middle phalanx and articular surface of the navicular bone help indicate true joint pathology. Additional radiographical views can be used for the evaluation of distal and middle phalangeal osteophytes, such as the dorso-60°proximo45°-lateral-palmarodistomedial and opposite dorso-60°proximo45°-medial-palmarodistolateral oblique views (**Fig 1b**). This radiograph will highlight the dorsomedial and dorsolateral articular margins of the distal interphalangeal joint with minimal superimposition. No evidence of osteophytosis on these aspects of the articular margin helps confirm the pointed contour of the dorsodistal aspect of the middle phalanx as a normal variant.

Anatomic variations of the navicular bone have also been described, including variable thickness of the flexor cortex, parallel or convergent joint space between the navicular bone and distal phalanx, the shape of the central eminence, and a well-defined, crescent-shaped lucent region in the sagittal ridge (also known as central eminence) of the flexor surface observed on the palmaroproximal-palmarodistal (navicular skyline) view (Poulos *et al.* 1989; Kaser-Hotz and Ueltschi 1992; Becht *et al.* 2001). This focal lucent area has previously been described as a normal indentation or synovial fossa. A study of 48 forelimbs of Thoroughbred horses with radiography, computed tomography, histology and epifluorescence microscopy showed that the crescent-shaped lucent region is noncompact bone between a reinforcement line of compacted cancellous bone and the flexor cortex, resulting in a normal site of decreased mineralisation within the cortex (Berry *et al.* 1992) (**Fig 2**). The size and prominence of this lucent region will vary from horse to horse. Typically, the appearance is symmetrical between limbs on the same horse; however, that does require that radiographical projections are identical, as slight variation in the obliquity of the skyline view can affect how conspicuous the crescent lucency appears. The lateral radiographical view can also be of aid. Horses with a more prominent central lucency on the skyline view tend to have a more prominent concave curvature of the flexor cortex on the lateral view (Dyson 2011).

In contrast to the normal area of decreased bone density described above, erosions of the flexor cortex are classically rounded or ill-defined areas of osteolysis with variable

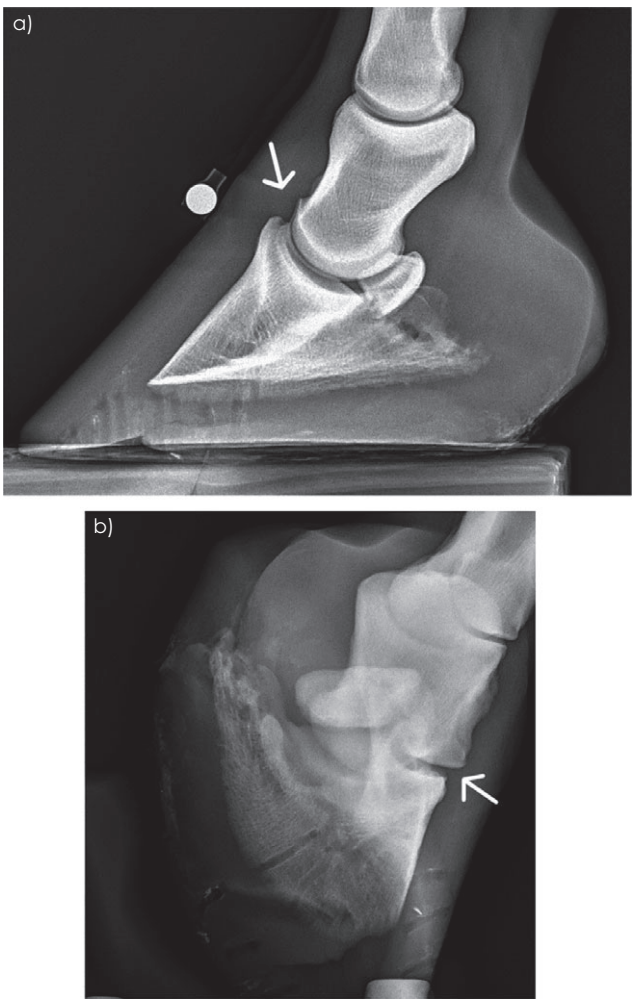

Fig 1: Lateromedial a) and dorso60°proximo45°lateral-palmarodistomedial oblique radiographical views b) of the distal interphalangeal joint of the same horse. On the lateral image, the extensor process of the distal phalanx and the dorsal distal aspect of the middle phalanx have sharp, pointed margins. There are no other signs of degenerative change associated with the distal interphalangeal joint, including the joint margins on the 60° oblique image. This dorsal contour is a normal variant for this horse.

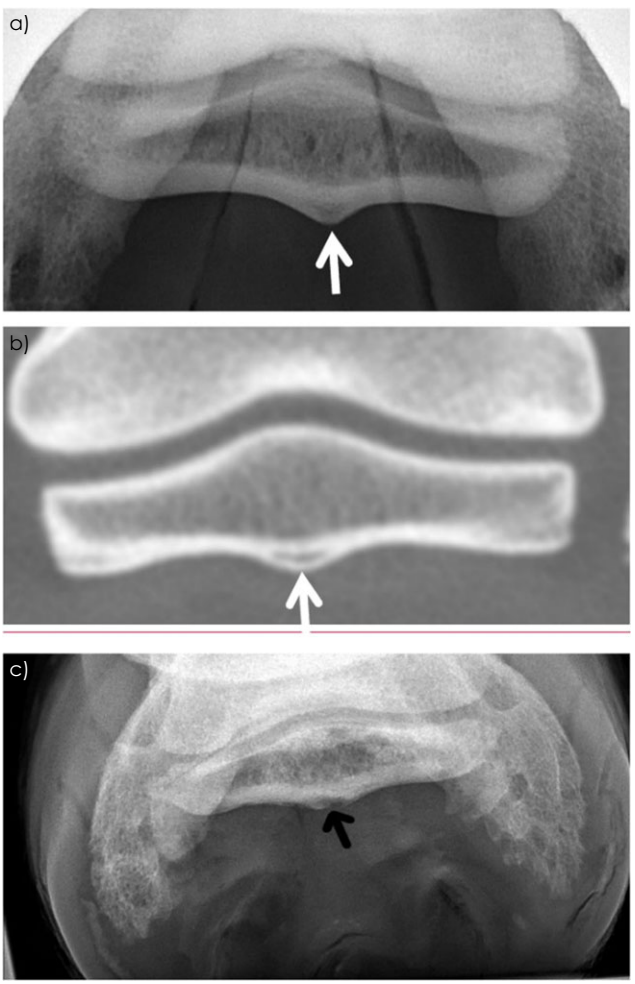

Fig 2: Palmaro55°proximal-palmarodistal (navicular skyline) radiographical view a) and transverse CT b) of the navicular bone. There is a normal focal area of decreased mineral in the sagittal ridge of the flexor surface. Gas packing artefact is incidentally present on the radiograph. c) For comparison: Pathological lysis of the flexor cortex at the sagittal ridge (black arrow), accompanied by other degenerative changes of the navicular bone including trabecular sclerosis.

amounts of endosteal sclerosis, which may result in a distinct concave radiolucent defect on the flexor surface. These radiographical features help differentiate the normal architecture of the navicular bone from a flexor erosion. Flexor cortex erosions are clinically relevant findings; therefore it is important that these normal lucent regions within the cortex are not overinterpreted and misdiagnosed as flexor cortical lysis. To achieve a diagnostic navicular skyline radiograph, multiple factors need to be considered including the position of the horse's limb, conformation, exposure and x-ray beam angle. A horse's limb should be placed caudally, behind the shoulder with the foot fully contacting the ground to achieve correct position of navicular bone relative to the middle and distal phalanges with a distinct separation between the middle phalanx and navicular bone. An upright foot conformation will require an increased beam angle in comparison to a flat foot. A recent study investigating the use of varying angles of the palmaroproximal-palmarodistal oblique (navicular skyline) radiograph found that a 35° view in conjunction with the standard 55° view improved radiographical detection of flexor cortical lysis (Johnson *et al.* 2018). Including additional navicular skyline projections of varying degrees can aid interpretation and result in a more accurate radiographical diagnosis.

Proximal and middle phalanges, proximal interphalangeal joint and fetlock

The distal aspects of the middle and proximal phalanges have a smooth, concave curvature between and proximal to the palmar aspect of the condyles, creating a central, rounded relative lucency on the dorsopalmar view (**Fig 3**). This region can sometimes be confused for a cyst-like lesion (Becht and Park 2000). In contrast to a true cyst-like

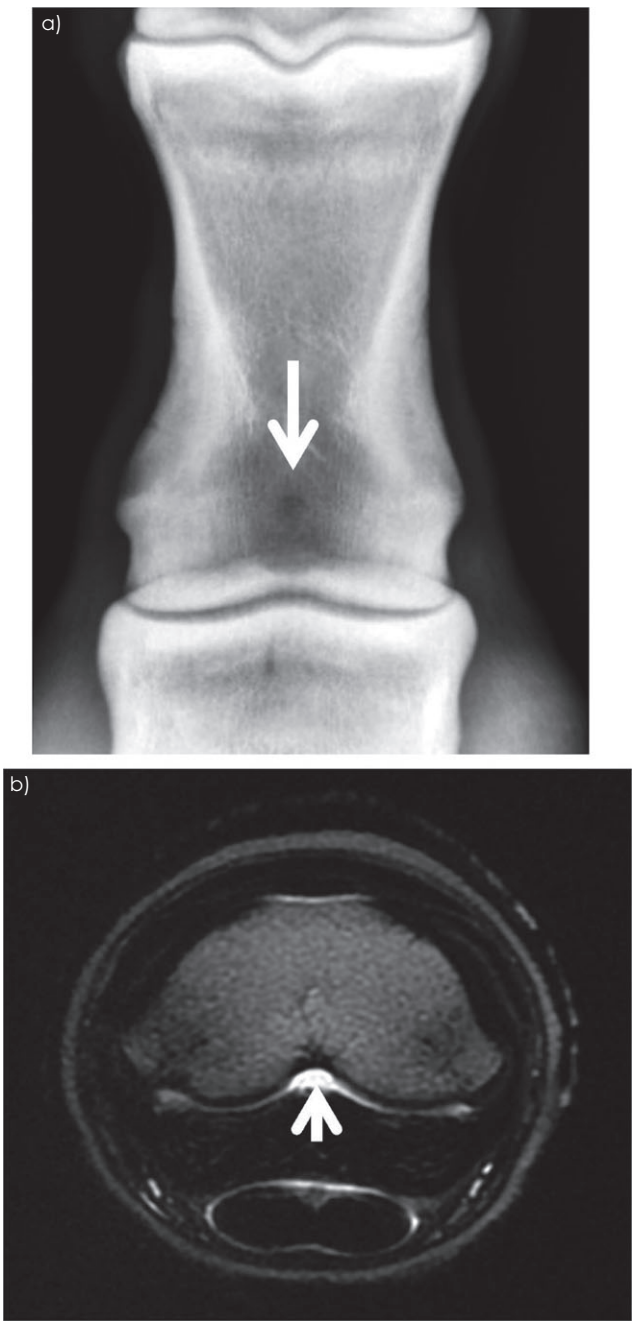

Fig 3: Dorsopalmar radiographical view of the pastern a) and transverse T2-weighted MRI of the distal aspect of the proximal phalanx b). The round ill-defined lucent region in the distal aspect of the proximal phalanx on the radiograph (long white arrow) corresponds with the normal palmar concavity of the proximal phalanx seen on the MRI (short white arrow). The linear lucent region in the mid aspect of the middle phalanx represents a nutrient foramen.

lesion, these relative lucent regions are not surrounded by sclerosis and do not have a concurrent subchondral bone defect. The prominence of this lucency will vary depending on patient conformation and the angle of the x-ray beam.

Carpus

The distal most aspect of the ulna (styloid process) has a separate centre of ossification from the distal radius. In juvenile horses, a well-defined lucent, linear to ovoid region extends obliquely between the distal radius and the separate centre of ossification of the styloid process of the ulna. In most horses, this will fuse completely. However, in some skeletally mature horses, there is incomplete closure of the ossification centre (**Fig 4**). This persistent lucent ovoid junction between the remnant ulna and radius can be mistaken for a fracture of the distal radius.

Another common area of confusion in the distal radius is the radial fossa (Becht and Park 2000). On the caudal aspect of the distal radius, there is a prominent, smooth indentation. This indentation appears as a round lucent area on the dorsopalmar view of the carpus and can be mistaken for a cyst-like lesion (**Fig 5**). Similar to the relative lucent region found in the proximal phalanx, this lucency can be distinguished from a cyst-like lesion due to the lack of surrounding sclerosis and lack of other evidence of joint disease. In advanced radiocarpal joint disease, this fossa can enlarge due to pressure resorption from chronic synovitis, creating even more of a cyst-like appearance.

In a group of 222 horses, investigators found several variations in the equine carpus, including the inconsistent presence of the first and fifth carpal bones. The first carpal bone and fifth carpal bone were found in 29% and 1.4% of limbs respectively (Simon and Dyson 2010). In some horses, the first carpal bone does not separate from the second carpal bone completely, resulting in an oblong and irregular palmar surface of the second carpal bone (**Fig 6**). The inconsistent appearance and presence of these carpal bones can result in misdiagnosis of pathological osseous fragmentation. Additionally, the fossa of the first carpal bone within the second carpal bone can be quite prominent. This can occur whether or not the first carpal bone is present and should not

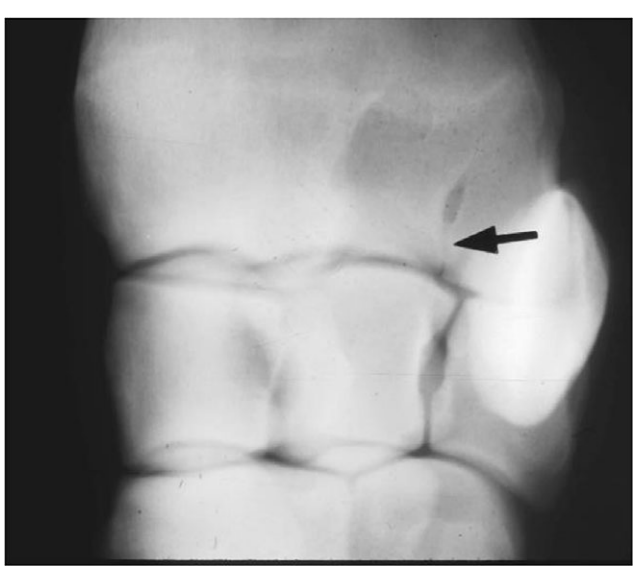

Fig 4: Dorsolateral-palmaromedial oblique radiographical view of the carpus. There is a persistent, well-defined lucent ovoid region and line between the distal radius and the incompletely ossified separate centre of ossification for the styloid process of the ulna (black arrow).

Fig 5: Dorsopalmar radiographical view of the carpus. The radial fossa has a prominent lucent zone in the central aspect of the distal radius. The prominence of this appearance will vary with x-ray beam angle and from horse to horse.

be mistaken for a cystic lesion within the second carpal bone. Importantly, while the presence of a first carpal bone is typically bilateral, the degree of irregularity or concave defect of the second carpal bone is variable and often asymmetric or unilateral; therefore, comparison to the opposite limb should not be relied upon to distinguish whether this is a normal or abnormal finding (Simon and Dyson 2010).

Elbow

The equine elbow is a region of few anatomic variations. Altered appearance of radiographical anatomy is more likely due to variation in radiographical position rather than true differences in gross anatomy (Dyson 1986). A common site of misinterpretation is the radioulnar articulation and the interosseous space between the ulna and radius (**Fig 7**). The superimposed undulating and irregular surfaces of the radial notch and the ulna at the level of the coronoid processes can be mistaken for a fracture or bone lysis in the mediolateral image. As with many of these variations, comparison with the contralateral limb can be performed to help clarify the normal heterogeneity of the bone at this site.

The radial head has prominent medial and lateral eminences at the attachment of the collateral ligaments. This is often mistaken as enthesopathy of the medial collateral ligament when observed on the craniocaudal view (Dyson 1986). The normal eminence is well-defined and smoothly marginated. In contrast, enthesopathy of the medial collateral ligament is relatively uncommon and typically results in bone roughening and bone spur formation (**Fig 8**).

Shoulder

The glenoid notch of the scapula has a concave margin that creates an ovoid lucent region on the cranial aspect of the

Fig 6: Dorsomedial-palmaromedial oblique radiographical view of the carpus. There is incomplete separation of the first and second carpal bone, creating an irregular margin to the fossa on the second carpal bone (white arrow).

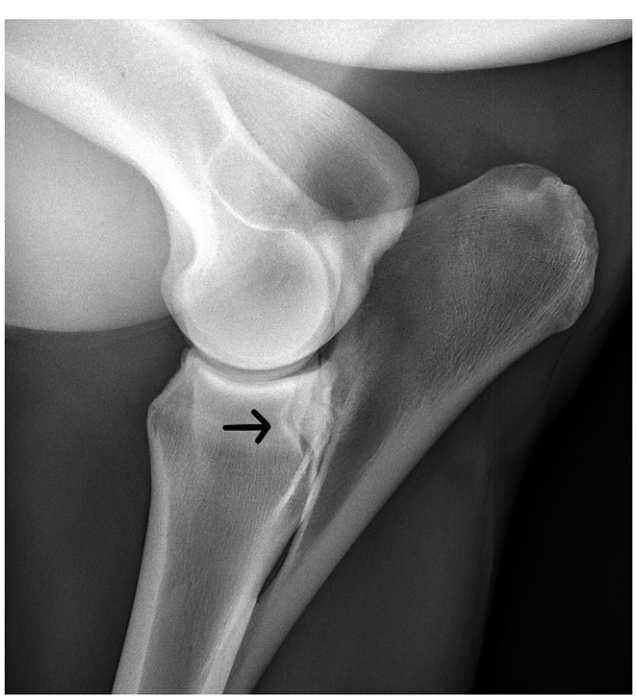

Fig 7: Mediolateral radiographical view of the elbow. There is an undulating lucent line at the radioulnar articulation and superimposition of the ulna (black arrow).

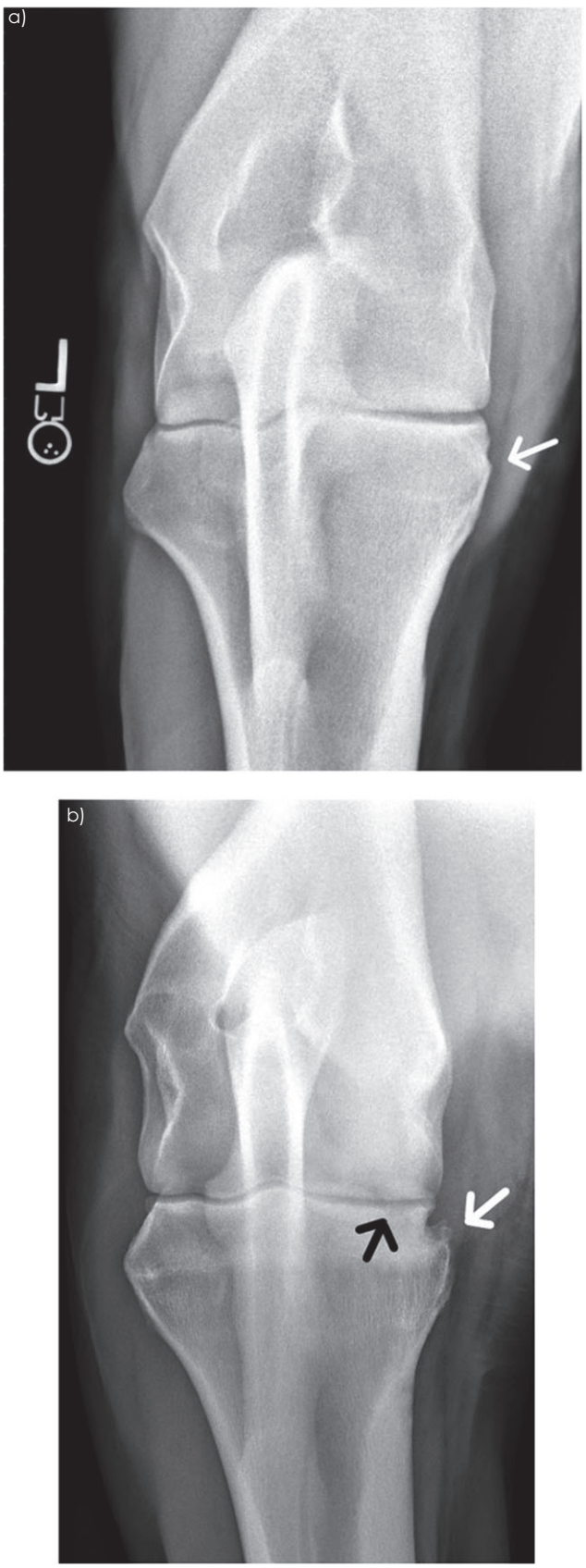

Fig 8: Craniocaudal radiographical views of the elbow in two different horses for comparison of normal anatomy vs. pathological change. a) A normal adult horse elbow with a medial eminence (white arrow). b) Smooth, triangular osseous proliferation on the proximal medial aspect of the radius consistent with medial collateral ligament enthesopathy of the elbow joint (white arrow). In addition, sclerosis of the medial humeral condyle and medial proximal radius is present with an ill-defined ovoid lucent region at the articular margin, consistent with a subchondral cyst-like lesion of the proximomedial radius (black arrow).

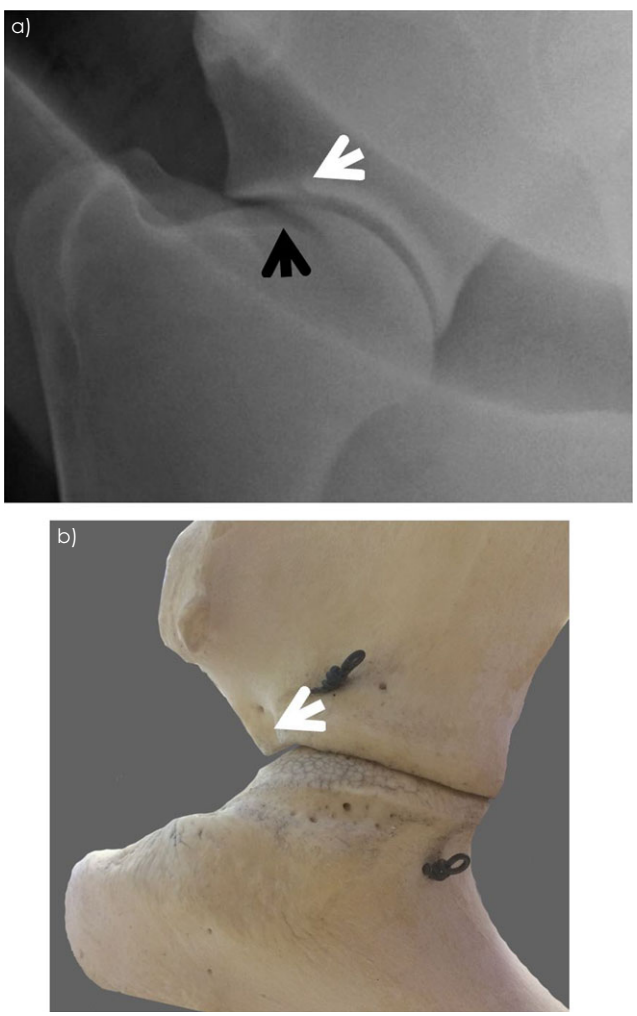

Fig 9: a) Mediolateral radiographical view of the shoulder. There is a lucent area within the cranial glenoid of the scapula due to the normal depression of the glenoid notch (white arrow), which corresponds to the labelled anatomic specimen. A second lucent line at the junction between the glenoid and the humeral head (black arrow). b) Anatomic specimen. The glenoid notch (white arrow) on the medial aspect of the glenoid of the scapula.

distal scapula that can be mistaken for a subchondral bone defect or cyst-like lesion (**Fig 9**). A second site of overinterpretation is a lucent zone at the junction of the glenoid cavity of the scapula and the humeral head that is often mistaken as subchondral cyst or fracture. This lucent zone is due to the medial rim of the glenoid being projected

more proximally than the lateral rim (Dyson 1986; Redding and Pease 2010). In contrast, osteochondrosis lesions of the shoulder joint more typically occur on the caudal aspect of the shoulder with accompanying sclerosis and articular surface irregularity.

Tarsus

Previous studies have shown that the distal aspect of the medial trochlear ridge of the talus is a common site of misinterpretation, in large part due to the variability in shape (Shelly and Dyson 1984; McIlwraith *et al.* 1991). The distal aspect can be rounded, pointed, or even a separate osseous body. The separate osseous bodies are often referred to as 'dew drop' lesions and are an incidental normal variation (McIlwraith *et al.* 1991). The mid dorsal aspect of the medial trochlear ridges of the talus can be variably flattened to focally concave. Apart from rare cases with concurrent subchondral bone sclerosis or fragmentation, this is an incidental variant and should not be confused with osteochondrosis (**Fig 10**).

Stifle

In juvenile horses, the trochlear ridges of the femur have irregular articular margins, which can persist until approximately 5 months of age (Adams and Thiisted 1985). The irregularity should be confined to the articular surface without evidence of bony lysis within the trabecular subchondral bone (**Fig 11**). When joint sepsis is suspected, the irregularity of the trochlear ridges and varying degree of ossification of the patella can be challenging to interpret. Radiographs of the contralateral limb can be helpful in differentiating normal juvenile bone irregularity from bone lysis associated with sepsis.

The medial femoral condyle has a normal variation in shape from rounded to flattened on the caudocranial view (Jeffcott 1984) and the appearance can be affected by x-ray beam angle. A flat medial femoral condyle articular surface in the absence of subchondral bone defects or sclerosis is an incidental variant. A slight concavity on the caudocranial view is of variable significance, is not necessarily an incidental finding and deserves further exploration. A flexed lateral oblique view of the stifle can be incorporated into the stifle study to provide improved visualisation of the weight-bearing aspect of the medial femoral condyle and more completely assess for pathological changes at this site. This radiographical projection can help detect more subtle lesions that might otherwise be missed on the caudocranial or caudolateral oblique view or demonstrate that what looks like a small defect on the caudocranial view is actually a more substantial articular surface defect (Barrett and Selberg 2012).

Cervical spine

The C6-7 articular process joints are unlike the cranial and mid-cervical spine articular process joints. The sixth cervical

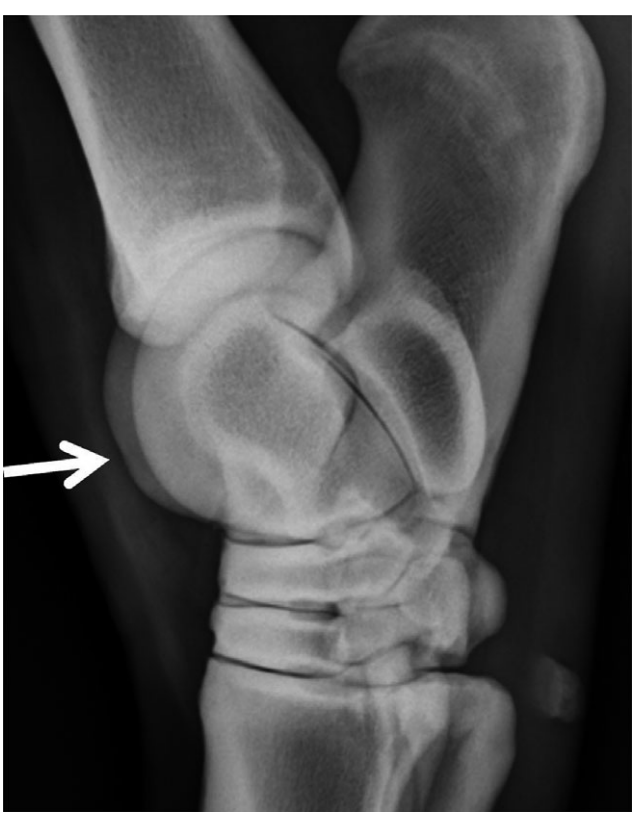

Fig 10: Lateromedial radiographical view of the tarsus with a flat contour to the dorsal aspect of the medial trochlear ridge (white arrow). There is no subchondral bone sclerosis or fragmentation, thus this is considered a normal anatomic variant.

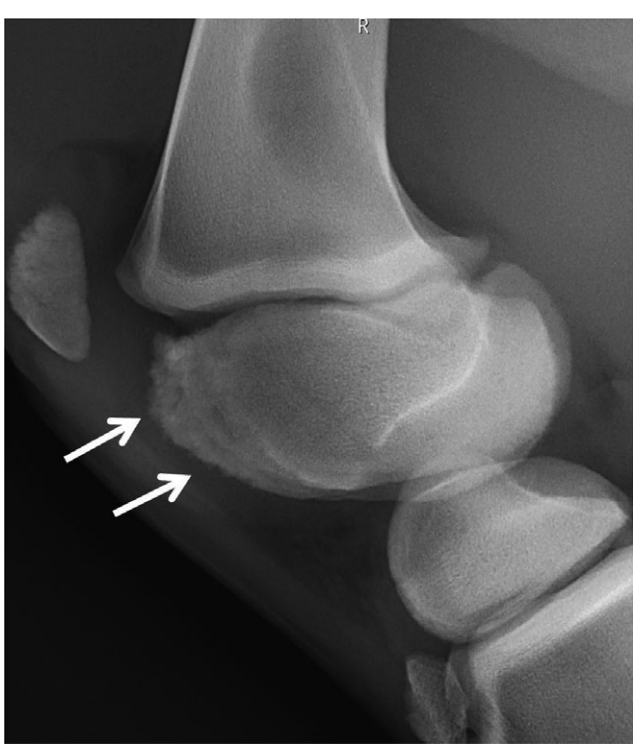

Fig 11: Lateromedial view of the stifle in a normal 3-week-old foal. The trochlear ridges are irregular and undulating (white arrows), consistent with the described appearance of a normal foal <5 months of age.

vertebra has shorter, thicker caudal articular processes that are situated further laterally. Correspondingly, the cranial articular processes of the seventh cervical vertebrae are wider and longer (Getty 1975). Consequently, these C6-7 articular process joints are normally more rounded and larger than the articular process joints in the cranial cervical spine. In addition to the anatomically normally larger articular process joints at C6-7, these articular process joints frequently undergo modelling and enlargement, which can be clinically insignificant. Although challenging to obtain, right 55° dorsal-left ventral and left 55° dorsal-right ventral oblique radiographs of the cervical articular process joints can aid in differentiation between bilateral and unilateral changes with improved evaluation of the articular process joints with decreased osseous superimposition.

Recent work has investigated the morphological radiographical variation in the sixth and seventh cervical vertebrae and the first thoracic vertebra in 270 horses. This group found the spinous process of the seventh cervical vertebra was identifiable in 76.1% of horses with described shape variations, including sharp triangle, rounded triangle, or spur-like shape (Santinelli *et al.* 2016). The spinous process of the seventh cervical vertebrae is partially superimposed with the dorsal aspect of the C6-7 articular process joints and can be mistaken for osteophyte formation and osteoarthritis (**Fig 12**).

A separate centre of ossification of the caudal aspect of the transverse process of the sixth cervical vertebra can be present in juvenile horses. In one review of a large equine population, this separate centre of ossification was only found in 4.8% of horses, the majority of which was <3 years of age (Santinelli *et al.* 2016). This physis remains open until 4–5 years of age and should not be confused for a fracture (Whitwell and Dyson 1987).

Thoracic spine

The cartilaginous summits of the thoracic spinous processes of T2 through T8 are not ossified in the newborn foal and begin to ossify around 12 months of age (Jeffcott 1979). These separate centres of ossification are commonly heterogeneously mineral with irregular margins and remain separate from the parent bone for the horse's lifetime. These normal separate centres can be distinguished from traumatic fractures by their alignment with the adjacent spinous processes and lack of other osseous abnormalities of the withers.

The thoracolumbar spinous processes and interspinous spaces are common areas of evaluation in prepurchase examinations and insurance claims (Penell *et al.* 2005). The standard grading scales are based on interspinous distances of <4 mm indicating pathological abnormalities. This is dependent on the age of the horse as the interspinous distances decrease with age (Jeffcott 1979). In Thoroughbred horses, the summits of the spinous processes tend to be beak-shaped with narrower interspinous spaces, which can predispose Thoroughbreds to spinous process impingement. (Jeffcott 1979). Patient positioning, x-ray beam angle and geometric distortion have also been proven to have significant effect in interspinous distances (Berner *et al.* 2012; Djernaes *et al.* 2017).

Horses are commonly sedated for spinal radiographs and head position becomes low, resulting in flexion of the cranial thoracic spine and extension of the caudal thoracic spine (Álvarez *et al.* 2006). The interspinous distances between eighth and 14th spinous processes were significantly wider in a low head position compared with intermediate (neutral) and high head positions. The 15th–17th interspinous distances were significantly wider in the low head position compared with the high head position, but not significantly different than the intermediate head position. In the high head position, variable interspinous distances were significantly narrowed compared with the intermediate head position (Berner *et al.* 2012).

A recent study also found x-ray beam angle to make a significant difference in interspinous space measurements. If

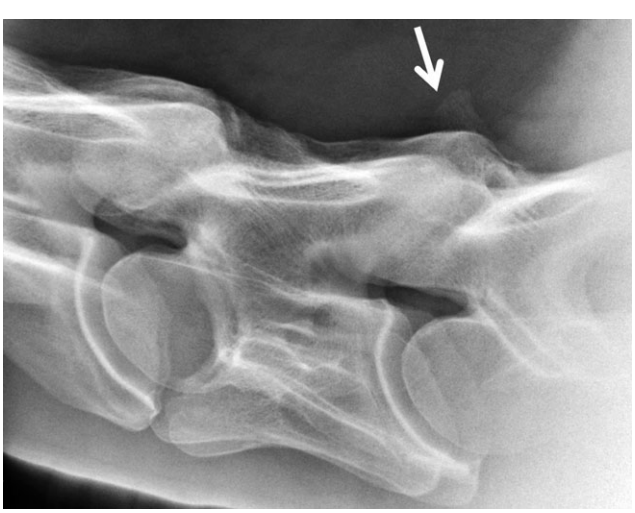

Fig 12: Lateral radiographical view of the caudal cervical spine. There is a prominent, triangular spinous process of C7 (white arrow).

Fig 13: Lateromedial radiographical view of the proximal phalanx with a dorsally located vascular channel (white arrow).

the interspinous space being evaluated was three spaces caudal to the centre of the x-ray beam, the measurement of the interspinous space of interest was significantly different compared with measurements of this space when centred in the radiographs or in closer positions (one or two spaces away from centre) (Djernaes *et al.* 2017). Interestingly, this difference in width did not have a consistent pattern and could not be predicted. Attempting to evaluate an interspinous space at a distant site (edge of film) will lead to geometric distortion, thus the reason for significantly different measurements. Concurrent osseous abnormalities, such as cortical lysis and sclerosis of the spinous processes, can help confirm true spinous process impingement when present. For these reasons, veterinarians acquiring spinal radiographs should be cognisant of head position and x-ray beam angle creating limitations when interpreting this region. A neutral head position with the spinous processes of concern centred in the x-ray beam is advised for the best quality diagnostic radiographs and ease of interpretation.

Nutrient foramina

While most practitioners are familiar with the common locations of the nutrient foramina within the long bones and phalanges, there are some nutrient foramina that are not consistently present in all horses and are often not bilaterally symmetric. These less commonly visualised nutrient foramina can be easily mistaken for a fracture, particularly in patients with acute onset of severe lameness in which a fracture is suspected. Common areas of misinterpretation include a variable present dorsal foramina in the proximal phalanx (Kneller and Losonsky 1990; Smith 1996) (**Fig 13**). Smaller foramina are also seen extending from the more prominent nutrient foramen in the metacarpus. Nutrient foramina are cylindrical lucent regions with well-defined thin opaque linear borders on either side of the foramen. In contrast, fracture margins can be sharp, but not cylindrical and do not have a thin, symmetric line of surrounding opacity. The typical radiographical appearance of a nutrient foramen may aid in differentiating a nutrient foramen from a fracture. In cases where it is unclear if a linear lucent area in the bone is a normal foramen or a fracture, the patient should be confined with repeat radiographs obtained in 7–10 days. A nutrient foramen will not alter in appearance, whereas a fracture will have widening of the fracture margins and progressive surrounding sclerosis.

Conclusions

In summary, there are multiple radiographical variants associated with normal conformational or anatomic variations. Recognising these normal variants is essential to avoid inappropriate radiographical interpretation and subsequent improper case management. Understanding normal anatomy, radiographical signs of disease and engaging in collaboration with veterinary colleagues will maximise accurate radiographical interpretation and minimise the risk of misdiagnosis.

Authors' declaration of interests

No conflict of interest has been declared.

Ethical animal research

Literature review with appropriate citations. All images were obtained from previous, unidentified case archives or client owned animals who gave consent for diagnostics to be used in research studies. This article neither directly impacted these animals in diagnoses nor in outcome.

Authorship

M. Barrett contributed to the study design, study execution, data analysis and interpretation, and preparation of the manuscript. F. Hinkle, S. Johnson and K. Selberg contributed to the study execution, data analysis and interpretation, and preparation of the manuscript. All the authors gave their approval of the final manuscript.

References

Adams, W.M. and Thiisted, J.P. (1985) Radiographic appearance of the equine stifle from birth to 6 months. *Vet. Rad.* **26**, 126-132.

Álvarez, C.B.G., Rhodin, M., Bobbert, M.F., Meyer, H., Weishaupt, M.A., Johnston, C. and Weeren, P.R. (2006) The effect of head and neck position on the thoracolumbar kinematics in the unridden horse. *Equine Vet. J.* **38**, *Suppl*. **36**, 445-451.

Barrett, M.F. and Selberg, K.T. (2012) How to obtain flexed lateral oblique radiographs of the equine stifle, *Proc. Am. Assoc. Equine Practnrs*, **58**, 383-387.

Becht, J.L. and Park, R.D. (2000) A review of selected normal radiographic variation of the equine fetlock, carpus, tarus, and stifle, *Proc. Am. Assoc. Equine Practnrs*, **46**, 362-364.

Becht, J.L., Park, R.D., Kraft, S.L., Steyn, P.F. and Wrigley, R.H. (2001) Radiographic interpretation of normal skeletal variations and pseudolesions in the equine foot. *Vet. Clin. North Am. Equine Pract.* **17**, 1-18.

Berner, D., Winter, K., Brehm, W. and Gerlach, K. (2012) Influence of head and neck position on radiographic measurement of intervertebral distances between thoracic dorsal spinous processes in clinically sound horses. *Equine Vet. J.* **44**, *Suppl*. **43**, 21-26.

Berry, C.R., Pool, R.R., Stover, S., O'Brien, T.R. and Koblik, P.D. (1992) Radiographic/morphologic investigation of a radiolucent crescent within the flexor central eminence of the navicular bone in thoroughbreds. *Am. J. Vet. Res.* **53**, 1604-1611.

Djernaes, J.D., Nielsen, J.V. and Berg, L.C. (2017) Effects of X-ray beam angle and geometric distortion on width of equine thoracolumbar interspinous spaces using radiography and computed tomography-a cadaveric study. *Vet. Radiol. Ultrasound.* **58**, 169-175.

Dyson, S. (1986) Interpreting radiographs 7: radiology of the equine shoulder and elbow. *Equine Vet. J.* **18**, 352-361.

Dyson, S. (2011) Radiological interpretation of the navicular bone. *Equine Vet. Educ.* **23**, 73-87.

Getty, R. (1975) *In: Sisson and Grossman's: the Anatomy of the Domestic Animals*, W B Saunders Co, St. Louis. p 258.

Jeffcott, L.B. (1979) Radiographic features of the normal equine thoracolumbar spine. *Vet. Rad.* **20**, 140-147.

Jeffcott, L.B. (1984) Interpreting radiographs 3: radiology of the stifle joint of the horse. *Equine Vet. J.* **16**, 81-88.

Johnson, S.A., Barrett, M.F. and Frisbie, D.D. (2018) Additional palmaroproximal-palmarodistal oblique radiographic projections improve accuracy of detection and characterization of equine flexor cortical lysis. *Vet. Radiol. Ultrasound.* **59**, 387-395.

Kaser-Hotz, B. and Ueltschi, G. (1992) Radiographic appearance of the navicular bone in sound horses. *Vet. Radiol. Ultrasound.* **33**, 9-17.

Kneller, S.K. and Losonsky, J.M. (1990) Variable locations of nutrient foramina of the proximal phalanx in forelimbs of Thoroughbreds. *J. Am. Vet. Med. Assoc.* **197**, 736-738.

McIlwraith, C.W., Foerner, J.J. and Davis, D.M. (1991) Osteochondritis dissecans of the tarsocrural joint: results of treatment with arthroscopic surgery. *Equine Vet. J.* **23**, 155-162.

Penell, J.C., Egenvall, A., Bonnett, B.N., Olson, P. and Pringle, J. (2005) Specific causes of morbidity among Swedish horses insured for veterinary care between 1997 and 2000. *Vet. Rec.* **157**, 470-477.

Poulos, P.W., Brown, A., Brown, E. and Gamboa, L. (1989) On navicular disease in the horse. *Vet. Rad.* **30**, 54-58.

Redding, W.R. and Pease, A.P. (2010) Imaging of the shoulder. *Equine Vet. Educ.* **22**, 199-209.

Santinelli, I., Beccati, F., Arcelli, R. and Pepe, M. (2016) Anatomical variation of the spinous and transverse processes in the caudal cervical vertebrae and the first thoracic vertebra in horses. *Equine Vet. J.* **48**, 45-49.

Shelly, J. and Dyson, S. (1984) Interpreting radiographs 5: radiology of the equine hock. *Equine Vet. J.* **16**, 488-495.

Simon, V. and Dyson, S.J. (2010) Radiologic anatomic variation of the carpus in horses with carpal lameness and control horses. *Vet. Radiol. Ultrasound.* **51**, 601-606.

Smith, R.K.W. (1996) Radiography of the equine metacarpo-/metatarsophalangeal joint. *Equine Vet. Educ.* **8**, 221-229.

Whitwell, K.E. and Dyson, S. (1987) Interpreting radiographs 8: equine cervical vertebrae. *Equine Vet. J.* **19**, 8-14.